

Interference effects due to commensurate electron trajectories and topological crossovers in (TMTSF)₂ClO₄

Authors: H.I. Ha, A.G. Lebed, Michael Naughton

Persistent link: <http://hdl.handle.net/2345/bc-ir:107156>

This work is posted on [eScholarship@BC](#),
Boston College University Libraries.

Published in *Physical Review B - Condensed Matter and Materials Physics*, vol. 73, no. 3, 2006

©2006 The American Physical Society. These materials are made available for use in research, teaching and private study, pursuant to U.S. Copyright Law. The user must assume full responsibility for any use of the materials, including but not limited to, infringement of copyright and publication rights of reproduced materials. Any materials used for academic research or otherwise should be fully credited with the source.

Interference effects due to commensurate electron trajectories and topological crossovers in $(\text{TMTSF})_2\text{ClO}_4$

H. I. Ha,^{1,*} A. G. Lebed,^{2,†} and M. J. Naughton¹¹*Department of Physics, Boston College, Chestnut Hill, Massachusetts 02467, USA*²*Department of Physics, University of Arizona, Tucson, Arizona 85721, USA*

(Received 21 November 2005; published 30 January 2006)

We report angle-dependent magnetoresistance measurements on $(\text{TMTSF})_2\text{ClO}_4$ that provide strong support for a macroscopic quantum phenomenon, the “interference commensurate” (IC) effect, in quasi-one dimensional metals. In addition to observing rich magnetoresistance oscillations, and fitting them with one-electron calculations, we observe a clear demarcation of field-dependent behavior at local resistance minima and maxima (versus field angle). Anticipated by a theoretical treatment of the IC effect in terms of Bragg reflections in the extended Brillouin zone, this behavior results from one-dimensional \rightarrow two dimensional (1D \rightarrow 2D) topological crossovers of electron wave functions as a function of field orientation.

DOI: [10.1103/PhysRevB.73.033107](https://doi.org/10.1103/PhysRevB.73.033107)

PACS number(s): 72.15.Gd, 71.18.+y, 74.70.Kn

In recent years, several types of angular magnetoresistance oscillation (AMRO) phenomena have been discovered in quasi-one dimensional metals such as the organic conductors $(\text{TMTSF})_2\text{X}$.¹ Such materials can be envisioned by considering one’s hand. The fingers represent highly conducting chains along x that are weakly coupled within the hand along y , forming a conducting layer with in-plane anisotropy. The hands are themselves coupled even more weakly along z , forming a highly anisotropic, three-dimensional (3D) system. The AMRO effects occur when a magnetic field is rotated within different planes in this system.

For example, y - z plane field rotations in $(\text{TMTSF})_2\text{ClO}_4$ ²⁻⁵ and $(\text{TMTSF})_2\text{PF}_6$ ^{6,7} reveal the Lebed⁸ “magic angle” effect, wherein the interlayer (interhand) resistivity develops pronounced minima at characteristic orientations given by $N(b/c)\tan\theta=1$, where N is an integer, $b//y$ and $c//z$ are interchain (interfinger) and interplane (interhand) crystal spacings, respectively, and θ is the tilt angle from b to c . Resonant oscillations up to ~ 10 th order in N have been observed to date.⁹ As first shown by Danner, Kang, and Chaikin (DKC),¹⁰ rotating in the x - z plane results in the appearance of a single resistivity peak centered about a small tilt angle from $B//x$ (from the fingers). Finally, rotations from x to y (within the plane of the hand) result in the “third angular effect” (TAE) which is manifest as a resistance minimum near $B//x$.¹¹⁻¹³

There have been many proposed explanations of the y - z plane magic angle effect,^{8,14-17} including some involving interactions between electrons.^{7,8,16} While these theories share many common aspects, a consensus is still lacking. There even exists experimental evidence⁷ of a non-Fermi liquid origin to some magic angle effects. The x - z plane effect is simpler to understand, being tied directly to details of the warped open Fermi surface. Through this effect, the transfer integral ratio t_b/t_a may be measured.¹⁰ Since $t_a \sim E_F$, the Fermi energy, and can be independently determined, this effect provides a means to measure t_b , the interchain coupling, or the degree to which the Fermi sheets are warped in the k_b direction. Other viewpoints based on the Boltzmann kinetic equation and weak incoherent electron transport perpendicu-

lar to the conducting planes are discussed in Refs. 18 and 19. The x - y plane TAE is ascribed to the velocity-preserving nature of “effective” electrons, via their proximity to geometrical inflection points on the Fermi surface.²⁰ As such, this can be used to quantify the interplane coupling t_c as well as t_b . These latter two AMRO effects result, to varying degrees, from the semiclassical behavior of electrons on a warped, open Fermi surface in a magnetic field, and can be explained by solving the Boltzmann kinetic equation in one Brillouin zone.^{10,20}

When one rotates a magnetic field through something other than one of these principal planes, the simplest expectation is for some trivial combination of the above three AMRO effects. In fact, in the first such experiment¹³ on $(\text{TMTSF})_2\text{PF}_6$, x - y plane rotations with a finite field component along z , a rich AMRO spectrum was observed. These so-called “LN oscillations” were first interpreted in the simple manner above, with resistivity minima ascribed to projections of commensurate directions according to $N(b/c)\tan\theta=\sin\phi$ (N =integer and ϕ is the tilt angle from a to b).¹³ However, it has recently been suggested via analytical theory that the origin of these complex oscillations is instead related to interference effects due to commensurate electron trajectories in a tilted magnetic field in the extended Brillouin zone.^{21,22} Moreover, as shown in Ref. 22, the interference commensurate (IC) effect leads to topological 1D \rightarrow 2D crossovers at commensurate directions of a magnetic field. In this Report, we provide evidence for this IC interpretation in the sister compound $(\text{TMTSF})_2\text{ClO}_4$ via angle-dependent magnetoresistance measurements. We use the IC theory to accurately calculate the angle dependence, and we report a new manifestation of the IC effect in fixed-angle experiments, where the magnetoresistance displays qualitatively different behavior at field orientations when the resistance is at a local maximum versus a minimum, corresponding to 1D and 2D transport, respectively.

The $(\text{TMTSF})_2\text{X}$ ($\text{X}=\text{ClO}_4, \text{PF}_6$, etc.) family of organic conductors can be modeled more quantitatively by a tight-binding band approximation, with electron band energy given by $E_k=-2t_a \cos(k_a a/2)-2t_b \cos(k_b b)-2t_c \cos(k_c c)$.¹

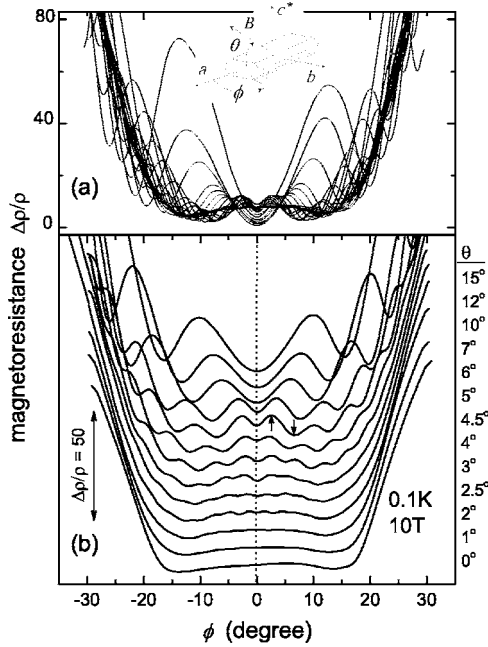


FIG. 1. (a) Raw data of interlayer magnetoresistance $\Delta\rho/\rho$ during a - b -plane ϕ -rotations for several c -axis magnetic field components θ between 0 and 20°, all at 0.1 K and 10 T. The curves have a common background resistance associated with the third angular effect. (Inset) Rotation angles θ and ϕ with respect to the crystal. (b) Subset of raw data, offset for clarity, with angles θ indicated at right.

With the strongest overlap of π -molecular orbitals along the a -direction (x , chain, finger), the electron energy E_k is mostly dominated by k_a and is nearly independent of k_b and k_c . Therefore, the Fermi surface consists of a pair of warped sheets, defined by the electron transfer energies t_a , t_b , and t_c along the three crystal axes. These latter two are the inter-finger and inter-hand couplings, respectively, discussed above. Because of the open Fermi surface, traditional magnetic oscillations²³ cannot exist in these materials. Nonetheless, the metallic phase of $(\text{TMTSF})_2\text{X}$ exhibits the large number of unconventional magnetic oscillations directly related to this open Q1D Fermi surface discussed above.

The geometry of our experiment is shown in the inset to Fig. 1. We show the two angles θ and ϕ , corresponding to magnetic field rotation directions out of and within the x - y (a - b) plane, respectively. Two $(\text{TMTSF})_2\text{ClO}_4$ crystals were mounted with 12 μm gold wires and graphite paste on an *in situ* θ -rotating stage of a dilution refrigerator, situated in a ϕ -rotatable split-coil superconducting magnet. The ϕ -dependence of the interlayer resistivity ρ_{zz} for various angles θ was measured at fixed temperature and field. The two samples showed nearly identical behavior; results for one are shown here. We show in Fig. 1(a) the magnetoresistance $[\rho(B) - \rho(0)]/\rho(0) \equiv \Delta\rho/\rho$ at 0.1 K and 10 T, where $\rho(0)$ is the extrapolated zero-field resistivity at 0.1 (i.e., ignoring the superconducting transition). For clarity, the same data are shown in Fig. 1(b) with vertical offsets. The bottom curve there represents a pure x - y or a - b plane rotation without any c -axis field component ($\theta=0$). The double minimum seen there, corresponding to the TAE, is distinctive up to

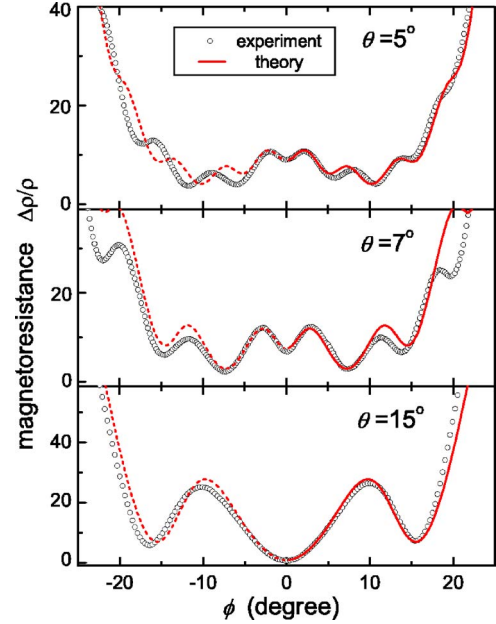


FIG. 2. (Color online) Angle-dependent magnetoresistance calculated for $\theta=5^\circ$, 7° , and 15° (lines) compared with the experimental data at 0.1 K, 10 T (open circles). The same fitting parameters were used for all three curves (see text), but only for positive angles (solid portions of lines).

small tilt angles, $\theta < \sim 3^\circ$, and is then slowly smeared out as richer (LN) oscillations develop at larger θ . The positions of these LN oscillation minima correspond to commensurate magnetic field directions²² $2N(b/c)\tan\theta = \sin\phi$, where the coefficient 2 is due to the reduced size of the Brillouin zone ($b \rightarrow 2b$) in $(\text{TMTSF})_2\text{ClO}_4$.

In the IC theory,^{21,22} the origin of the LN oscillations is related to special commensurate electron trajectories where the average electron velocity along z is nonzero. This analytical theory²¹ well describes previous data¹³ on $(\text{TMTSF})_2\text{PF}_6$ whereas, for the present case, a more complex approach is needed to account for the doubling of the unit cell along the b -axis due to ordering of the ClO_4 anions. The details of this approach are published elsewhere.²² The resulting conductivity, accounting for the anion ordering gap Δ_{AO} , is given by:

$$\sigma_{zz} \sim \int_{-\infty}^0 dt e^{t/\tau} \int_0^{2\pi} (dy/2\pi) \cos[\omega_c t + (\omega_c^*/\omega_b)] \times (\sqrt{\cos^2(\omega_b t + y) + A^2} - \sqrt{\cos^2 y + A^2}),$$

where $\omega_b = ev_F b B \sin\theta$, $\omega_c = ev_F c B \cos\theta \sin\phi$, $\omega_c^* = ev_y^0 c B \cos\theta \cos\phi$, $v_y^0 = 2t_b/b$, $y = k_y b$, and $A = \Delta_{\text{AO}}/2t_b$.

In Fig. 2, we compare the calculated conductivity using this formalism with the data of Fig. 1, using the same values of $t_a/t_b = 9.75$, $\omega_c \tau = 15$ at $B = 10$ T and $\Delta_{\text{AO}}/2t_b = 0.10$ for all three curves. While all three quantities were used as fitting parameters, the first was constrained by simultaneous fits to angle positions of DKC oscillations on the same sample, which depend very sensitively on this ratio t_a/t_b . For the second, the magnetic field and thus ω_c is fixed, so the vari-

able is the relaxation time τ . We found rather strong sensitivity to this quantity, with overall consistency of fits only for $\omega_c\tau=15\pm 0.5$, a value consistent with the literature.¹³ The resulting curves demonstrate not only qualitative but rather good quantitative agreement between theory and experiment over a broad range of magnetic field orientations. (The data are asymmetric with respect to zero angle ϕ , since the actual crystal structure is triclinic, while the calculations are for an orthorhombic approximation, with only positive angle data chosen for the fitting.)

The above suggests that the interference commensurate phenomenon may be an ideal tool to determine all band parameters in Q1D conductors, such as the in-plane anisotropy t_a/t_b and the anion ordering gap Δ_{AO} , and it can be also used for a determination of the nontrivial topology of a Fermi surface. Unlike $(\text{TMTSF})_2\text{PF}_6$, due to the anion ordering in $(\text{TMTSF})_2\text{ClO}_4$, not only is the size of the Brillouin zone reduced, but also the shape of the Fermi surface is changed. Thus, when the magnetic field is applied, the electron trajectories in these two systems are quite different. Especially in the absence of any magnetic breakdown, electrons travel on only one part of the Fermi surface in $(\text{TMTSF})_2\text{ClO}_4$. Note that the positions of the LN oscillation minima are defined only by the dimensionality of electron wave functions in the magnetic field and correspond to the condition²² $2N(b/c)\tan\theta=\sin\phi$ in $(\text{TMTSF})_2\text{ClO}_4$. Thus, the shape and amplitudes of the oscillations are affected by the shape of the FS such that, by their analysis, we can define the shape of the FS more accurately. In conventional metals²³ with closed Fermi surfaces, the dHvA effect is traditionally used to obtain the shape of the Fermi surface, but this cannot be done on open Fermi surfaces, as they appear in $(\text{TMTSF})_2\text{X}$. The present technique provides such capability.

The anion order gap parameter used in the above fits can be compared to a value extracted from magnetic breakdown across the anion gap, corresponding to ω_c of the order of Δ_{AO}^2/t_b . Using the Gor'kov-Lebed equations from Ref. 24, the probability of an electron orbit experiencing magnetic breakdown varies as $\exp(-\pi\Delta_{AO}^2/2t_b\omega_b)$. Using a breakdown field of 15 T from Yan *et al.*²⁵ yields $\Delta_{AO}=56$ K (for $t_b=200$ K and $\omega_c=1.5$ K/T), corresponding to a ratio $\Delta_{AO}/2t_b=0.14$. This is indeed comparable to the 0.10 ratio used in our fits above, which yielded an anion gap of $\Delta_{AO}\sim 40$ K, as well as to the value of 0.14 from Yoshino *et al.*²⁶ (or 0.17, depending on whether one uses our $t_a/t_b=9.75$, or their ratio of 12) from a study of the TAE under pressure. Analysis of these oscillations now provides a highly accurate way to determine this anion ordering gap.

The key point of this work, which was not appreciated in our earlier Report,²¹ is that the magnetoresistance oscillations in Figs. 1 and 2 can be interpreted in terms of unique one- to two-dimensional crossovers, with unique consequences. In the absence of Landau quantization for open Fermi surfaces, the "other" quantum effect in a magnetic field, Bragg reflections, results in a series of 1D to 2D crossovers at the LN oscillation minima. In other words, electron wave functions, localized on chains (i.e., 1D) at arbitrary field directions,^{8,16} become delocalized on planes (i.e., 2D) at the commensurate directions. The nontrivial physical origin

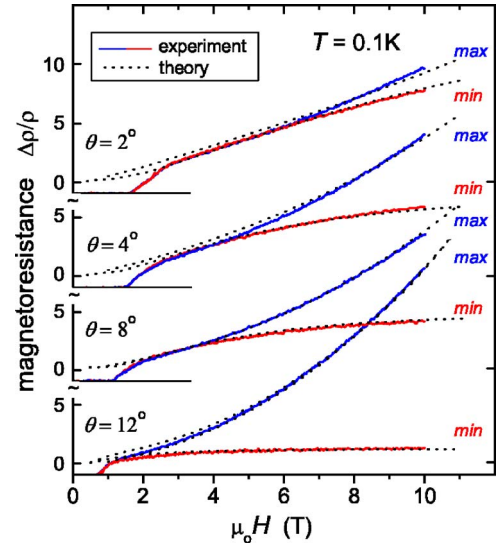


FIG. 3. (Color online) 1D \rightarrow 2D topological crossovers as revealed by $\Delta\rho/\rho(B)$ at certain commensurate and noncommensurate orientations. For each angle θ indicated, ϕ was adjusted to reach a resistance maximum or minimum, as represented by the set of arrows in the $\theta=6^\circ$ data in Fig. 1. For maxima (blue), the magnetoresistance is nonsaturating in field (1D-like), while for minima (red), it tends to saturation (commensurate, 2D-like). Consistent dependencies occur in the calculated magnetoresistance (ignoring the superconducting transition at low field), as shown in dashed lines atop each experimental curve.

of these 1D \rightarrow 2D crossovers is related to interference effects between velocity components along the z -axis, k_z , and electron motion along the y -direction.²² These interference effects occur as electrons move along open FS sheets in the extended Brillouin zone and are qualitatively different from that responsible for the magic angle effect.¹⁷ A discussion of how 1D \rightarrow 2D dimensional crossovers can lead to the appearance of oscillation minima in ρ_{zz} can be found in Ref. 22.

We can use this dimensional crossover notion and the IC model to further discuss electron motion in such quasi-1D metals in a strong magnetic field. For electrons localized on conducting x -chains, one expects, in the absence of impurities ($1/\tau=0$), the conductivity between chains σ_{zz} to be zero. For $1/\tau\neq 0$, σ is finite and should vary as $1/\omega_c^2\tau^2\sim 1/B^2$ at high field, when $\omega_c\gg 1/\tau$. If, at commensurate field directions, electron wave functions become delocalized (2D), then σ_{zz} is expected to be similar to conductivity in the absence of a magnetic field. Thus, σ_{zz} should saturate at high field and be proportional to τ . In other words, as a consequence of the 1D \rightarrow 2D crossovers, $\rho_{zz}(B, \theta, \phi)\equiv 1/\sigma_{zz}$ should saturate at high field for commensurate orientations, and tend toward B^2 behavior away from these special directions. This is in contrast to the conventional behavior of magnetoresistance in an open-orbit metal,²⁷ and the results of purely semiclassical calculations for $(\text{TMTSF})_2\text{X}$ materials that include finite interlayer hopping.²⁸ Figure 3 presents the results of field sweeps at several of the minima and maxima of our LN oscillation data of Figs. 1 and 2. As predicted, $\Delta\rho_{zz}/\rho(B, \theta, \phi)$ saturates at commensurate directions (minima), while at noncommensurate directions (maxima), it

exhibits nonsaturating behavior. As shown in Fig. 3, there is a rather good agreement between experiment and the calculated magnetoresistance using the conductivity equation above and the same parameters as were used for the fits in Fig. 2. Thus, the predicted dramatic difference between commensurate 2D and noncommensurate 1D magnetoresistance, with saturating at commensurate angles (minima in angle sweeps) and nontrivial, nonsaturating otherwise, is borne out in experiment and calculation.

In summary, Bragg reflections, which occur as electrons move along open Fermi surface sheets in an extended Brillouin zone in the quasi-1D metal (TMTSF)₂Clo₄, result in interference effects which represent a type of macroscopic quantum phenomenon in a magnetic field, of topological origin. Due to these interference effects, the effective space

dimensionality of the electron wave function is changed, resulting in large conductivity oscillations, with $\Delta\sigma/\sigma \gg 1$, far more than is observed to result from Landau quantization of electron orbits in conventional metals. We expect that the method suggested in this Report for determining the topology and shape of open Fermi surfaces will be found useful for other families of low-dimensional conductors (such as (DMET-TSeF)₂X, κ -(ET)₂Cu(NCS)₂, α -(ET)₂MHg(XCN)₄, etc.). It may as well be a reliable tool to test for Fermi-liquid behavior in (TMTSF)₂X conductors, which is claimed to be broken^{7,29} under certain experimental conditions.

This work was supported by NSF Grant No. DMR-0308973 and INTAS Grant No. 2001-0791. We would like to acknowledge Harukazu Yoshino for helpful discussions.

*Current address: Department of Physics, Harvard University, Cambridge, Massachusetts.

[†]Also at: L.D. Landau Institute for Theoretical Physics, Moscow, Russia.

¹T. Ishiguro, K. Yamaji, and G. Saito, *Organic Superconductors*, 2nd ed. (Springer-Verlag, Berlin, 1998).

²M. J. Naughton, O. H. Chung, L. Y. Chiang, and J. S. Brooks, *Mater. Res. Soc. Symp. Proc.* **173**, 257 (1990).

³T. Osada, A. Kawasumi, S. Kagoshima, N. Miura, and G. Saito, *Phys. Rev. Lett.* **66**, 1525 (1991).

⁴M. J. Naughton, O. H. Chung, M. Chaparala, X. Bu, and P. Coppens, *Phys. Rev. Lett.* **67**, 3712 (1991).

⁵G. S. Boebinger, G. Montambaux, M. L. Kaplan, R. C. Haddon, S. V. Chichester, and L. Y. Chiang, *Phys. Rev. Lett.* **64**, 591 (1990).

⁶W. Kang, S. T. Hannahs, and P. M. Chaikin, *Phys. Rev. Lett.* **69**, 2827 (1992).

⁷W. Wu, I. J. Lee, and P. M. Chaikin, *Phys. Rev. Lett.* **91**, 056601 (2003).

⁸A. G. Lebed, *Pis'ma Zh. Eksp. Teor. Fiz.* **43**, 137 (1986) [*JETP Lett.* **43**, 174 (1986)]; A. G. Lebed and P. Bak, *Phys. Rev. Lett.* **63**, 1315 (1989).

⁹H. Y. Kang, Y. J. Jo, S. Uji, and W. Kang, *Phys. Rev. B* **68**, 132508 (2003).

¹⁰G. M. Danner, W. Kang, and P. M. Chaikin, *Phys. Rev. Lett.* **72**, 3714 (1994).

¹¹H. Yoshino, K. Saito, K. Kikuchi, H. Nishikawa, K. Kobayashi, and I. Ikemoto, *J. Phys. Soc. Jpn.* **64**, 2307 (1995); H. Yoshino, K. Murata, K. Saito, H. Nishikawa, K. Kikuchi, and I. Ikemoto, *ibid.* **65**, 3127 (1996); H. Yoshino, K. Saito, H. Nishikawa, K. Kikuchi, K. Kobayashi, and I. Ikemoto, *ibid.* **66**, 2410 (1997).

¹²T. Osada, S. Kagoshima, and N. Miura, *Phys. Rev. Lett.* **77**, 5261

(1996).

¹³I. J. Lee and M. J. Naughton, *Phys. Rev. B* **57**, 7423 (1998); M. J. Naughton, I. J. Lee, G. M. Danner, and P. M. Chaikin, *Synth. Met.* **85**, 1481 (1997).

¹⁴T. Osada, S. Kagoshima, and N. Miura, *Phys. Rev. B* **46**, 1812 (1992).

¹⁵K. Maki, *Phys. Rev. B* **45**, 5111 (1992).

¹⁶A. G. Lebed, *J. Phys. I* **4**, 351 (1994); **6**, 1819 (1996).

¹⁷A. G. Lebed, N. N. Bagmet, and M. J. Naughton, *Phys. Rev. Lett.* **93**, 157006 (2004).

¹⁸R. H. McKenzie and P. Moses, *Phys. Rev. B* **60**, R11241 (1999).

¹⁹T. Osada and M. Kuraguchi, *Synth. Met.* **133-134**, 75 (2003).

²⁰A. G. Lebed and N. N. Bagmet, *Phys. Rev. B* **55**, R8654 (1997).

²¹A. G. Lebed and M. J. Naughton, *Phys. Rev. Lett.* **91**, 187003 (2003).

²²A. G. Lebed, H. I. Ha, and M. J. Naughton, *Phys. Rev. B* **71**, 132504 (2005).

²³A. A. Abrikosov, *Fundamentals of the Theory of Metals* (Elsevier, Amsterdam, 1988).

²⁴L. P. Gor'kov and A. G. Lebed, *Phys. Rev. B* **51**, 3285 (1995).

²⁵X. Yan, M. J. Naughton, R. V. Chamberlin, L. Y. Chiang, S. Y. Hsu, and P. M. Chaikin, *Synth. Met.* **27**, B145 (1988).

²⁶H. Yoshino, S. Shodai, and K. Murata, *Synth. Met.* **133-134**, 55 (2003).

²⁷A. B. Pippard, *Magnetoresistance in Metals* (Cambridge University Press, Cambridge, 1989).

²⁸H. Yoshino, Z. Bayindir, J. Roy, B. Shaw, H. I. Ha, A. Lebed, and M. J. Naughton, *Proc. ISCOM (6th Int'l Symp. Crystalline Organic Metals)*, Key West, FL, J. Low Temp. Phys. (unpublished).

²⁹G. M. Danner and P. M. Chaikin, *Phys. Rev. Lett.* **18**, 4690 (1995).